Earthquakes and Structures, *Vol. 9, No. 4 (2015) 875-891*
DOI: http://dx.doi.org/10.12989/eas.2015.9.4.875

Determination of critical excitation in seismic analysis of structures

Reza Kamgar and Reza Rahgozar*

Department of Civil Engineering, Faculty of Engineering, Shahid Bahonar University of Kerman, Kerman, Iran

(Received December 2, 2014, Revised April 28, 2015, Accepted May 3, 2015)

Abstract. Earthquake can occur anywhere in the world and it is essential to design important members in special structures based on maximum possible forces that can be produced in them under severe earthquake. In addition, since the earthquake is an accidental phenomena and there are no similar earthquakes, therefore the possibility of strong earthquakes should be taken into account in earthquake-resistant design of important structures. Based on this viewpoint, finding the critical acceleration which maximizes internal forces is an essential factor in structural design. This paper proposes critical excitation method to compute the critical acceleration in design of important members in special structures. These critical accelerations are computed so that the columns' internal shear force at the base of the structure at each time step is maximized under constraints on ground motion. Among computed critical accelerations (of each time step), the one which produces maximum internal shear force is selected. A numerical example presents to show the efficiency of critical excitation method in determining the maximum internal shear force and base moment under variety of constraints. The results show that these method can be used to compute the resonant earthquake which have large enough effective duration of earthquake strong motion (between 12.86 sec to 13.38 sec) and produce the internal shear force and base moment for specific column greater than the same value for selected earthquakes in constructing the critical excitation (for different cases about 2.78 to 1.29 times the San Fernando earthquake). Therefore, a group of them can be utilized in developing the response spectrum for design of special structures.

Keywords: linear dynamic response analysis; critical excitation method; belt truss system; shear force

1. Introduction

A great number of exact and approximate methods have been developed to investigate the behavior, deflection, vibration and modification of different types of tall buildings subjected to lateral loads (static or dynamic loading) over the past few decades (Kamgar and Saadatpour 2012, Kamgar and Rahgozar 2013, Heidari *et al*. 2014, Rahgozar and Sharifi 2009, Taranath 2012, Wu and Li 2003, Swaddiwudhipong *et al*. 2002, Kuang *et al*. 2004, Jahanshahi *et al*. 2012, Rahgozar *et al*. 2014, Malekinejad and Rahgozar 2014). After sever earthquakes, depending on the type of the structure, the damage must be eliminated or reduced. Therefore, it is necessary to have an

*Corresponding author, Professor, E-mail: rahgozar@mail.uk.ac.ir

http://www.techno-press.org/journals/eas&subpage=7 ISSN: 2092-7614 (Print), 2092-7622 (Online)

estimate of the maximum internal shear force and moment of base columns that can be produced in case of a severe earthquake.

Variability of ground motion is an important and challenging factor. Code-specified design ground motions are usually constructed by taking into account the knowledge from past observations and probabilistic insights. However, uncertainties in characteristics of earthquakes (or ground motions), the fault rupture mechanisms, the wave propagation mechanisms, the ground properties, etc. present serious difficulties in defining reasonable design ground motion; especially for important buildings in which severe damage or collapse must be avoided (Singh 1984, Anderson and Bertero 1987, Takewaki 2001a, 2002, 2013, Stein 2003). Critical excitation method is a promising robust technique in accounting for inherent uncertainties in earthquake characteristics and for constructing design earthquake ground motions in a reasonable way (Takewaki 2001b). In the field of structural engineering, robustness, redundancy and resilience play an important role in order to guarantee the safety of infrastructures against severe disturbances, e.g., earthquakes, strong winds, impacts (Takewaki 2013).

The method of critical excitation was proposed by Drenick (1970) for linear elastic, viscously damped single degree of freedom (SDOF) systems in order to take into account inherent uncertainties in ground motions. This method is aimed at finding the excitation which produces the maximum response from a class of allowable inputs. Drenick (1977) pointed out that the combination of probabilistic approach with worst-case analysis should be employed to make robust seismic resistant design. It was pointed out that the critical response based on Drenick's model is conservative. To resolve this point, Shinozuka (1970) discussed the same critical excitation problem in frequency domain. He proved that if an envelope function of Fourier amplitude spectra can be specified, a near upper bound of the maximum response can be obtained. Takewaki (2005) treated the earthquake input energy as the objective function in a new critical excitation problem. It has been shown that the formulation of the earthquake input energy in the frequency domain is essential for solving the critical excitation problem and deriving a bound on the earthquake input energy for a class of ground motions. Therefore, the frequency domain is used frequently by researchers (Fujita *et al.* 2014). Westermo (1985) considered the input energy during time acceleration divided by mass as the objective function in a new critical excitation model. His solution is not necessarily complete and explicit because the response velocity is actually a function of the excitation to be obtained (Takewaki 2013). Abbas (2006), Moustafa (2009), Moustafa (2011) studied the problem of modeling earthquake ground motions as design input for multi degree of freedom inelastic structures.

Finding the critical acceleration which maximizes internal forces (i.e., shear force, bending moment and so on) of important members, such as columns that their instability will lead to failure of the building, is an essential factor in structural design. The unexpected severe damage of infrastructure and buildings and the loss of lives during recent earthquakes as well as previous earthquakes have raised significant concern and questions on life safety and performance of engineering structures under possible future earthquakes (Moustafa 2012).

In this paper, maximum internal shear force and moment for columns at the base of the structure (referred as internal shear force and base moment) are determined. For this purpose, limited information on strong ground motion is assumed to be available at the given site. The design earthquake acceleration is expressed as a Fourier series, with unknown amplitude and phase angle, modulated by an envelope function. This method was presented by Moustafa (2011). The critical acceleration is computed by solving an inverse dynamic problem, using nonlinear programming technique, based on the available information from recorded ground motion so that the columns' internal shear force at the base of the structure is maximized. Amongst computed critical accelerations (from each time step), one which produces maximum internal shear force is selected.

As an example, a building which has been strengthened by a belt truss system is considered. This building is analyzed and designed using SAP 2000 program and allowable stress design (ASD 1989) method. In addition, since interior frames resist gravity loads while the exterior frames, strengthened by belt truss system, resist lateral loads and some part of the gravity loads, for critical excitation analysis only one of the exterior frames modeled as a two dimensional shear building under lateral loading is considered. Time history analysis is used and critical excitation based on constraints on ground motion at different times, between (0-T^*), is computed so that the internal shear force is maximized. From the set of these critical accelerations one which produces the maximum internal shear force is selected. Newmark β-method with ($\gamma = 1/2$ and $\beta = 1/6$) is used for time history analysis.

2. Critical excitation method for multi degree of freedom (MDOF) elastic structures

Moustafa (2011) introduced a method in construction of critical acceleration. He showed that ground acceleration can be represented as the product of Fourier series and an envelope function ($e(t) = A_0(\mathrm{e}^{-\alpha_1 t} - \mathrm{e}^{-\alpha_2 t}), \quad \alpha_2 > \alpha_1$) as follows

$$\ddot{u}_g(t) = A_0(\mathrm{e}^{-\alpha_1 t} - \mathrm{e}^{-\alpha_2 t})\sum_{i=1}^{N_f} R_i \cos(\omega_i t - \phi_i) \tag{1}$$

Where R_i and ϕ_i are the unknown amplitudes and phase angles, respectively, and ω_i $i = 1,2,...,N_f$ are frequencies present in the ground acceleration, selected to span the frequency range (for example 0.1 *to* 25 Hz). Moustafa (2011) expressed that it is also useful to select some of these frequencies to coincide with natural frequencies of the elastic structure, as well as placing relatively more points within the modal half-power bandwidth. In the envelope function, α_2 and α_1 are parameters that impact the observed transient trends in the recorded ground motion; and A_0 parameter is a scaling constant (Shinozuka and Sato 1967).

In constructing critical seismic inputs, the envelope function is assumed to be completely specified and R_i and ϕ_i parameters need to be computed. Furthermore, the information on energy *E,* peak ground acceleration (*PGA*) M_1, peak ground velocity (*PGV*) M_2, upper bound Fourier amplitude spectra (UBFS) $M_3(\omega)$, and lower bound Fourier amplitude spectra (LBFS) $M_4(\omega)$ are also assumed to be available. Abbas and Manohar (2002), Abbas (2006), proposed the following constraints

$$\begin{aligned} &\left[\int_0^{T^*} \ddot{u}_g^2(t)dt\right]^{\frac{1}{2}} \le E \qquad && \max_{0<t<T^*} \left|\ddot{u}_g(t)\right| \le M_1 \\ &\max_{0<t<T^*} \left|\dot{u}_g(t)\right| \le M_2 && M_4(\omega) < \left|\ddot{U}_g(w)\right| < M_3(\omega) \end{aligned} \tag{2}$$

Here T^* is duration of the earthquake and $\ddot{U}_g(w)$ is Fourier transform of the ground acceleration $\ddot{u}_g(t)$. In Eq. (2), the proposed constraint on earthquake energy is related to Arias intensity (Arias 1970). The UBFAS and the LBFAS constraints show the frequency content and amplitude of past recorded accelerograms for the design earthquake (Moustafa 2011). In fact, the problem is to find the unknown amplitudes and phase angles which maximize the objective function. To proceed further, it is needed to express the constraints in terms of Fourier coefficients R_i and ϕ_i. Constraints listed in Eq. (1) can be expressed in terms of the unknown variables as follows

$$\begin{aligned}
&\left[A_0^2\sum_{m=1}^{N_f}\sum_{n=1}^{N_f}R_mR_n\int_0^{\infty}(\mathrm{e}^{-\alpha_1\tau}-\mathrm{e}^{-\alpha_2\tau})^2\cos(\omega_m\tau-\phi_m)\cos(\omega_n\tau-\phi_n)\,d\tau\right]^{\frac{1}{2}}\le E\\
&\max_{0<t<T^*}\left|A_0(\mathrm{e}^{-\alpha_1 t}-\mathrm{e}^{-\alpha_2 t})\sum_{n=1}^{N_f}R_n\cos(\omega_n t-\phi_n)\right|\le M_1\\
&\max_{0<t<T^*}\left|A_0\sum_{n=1}^{N_f}\int_0^{t}R_n(\mathrm{e}^{-\alpha_1\tau}-\mathrm{e}^{-\alpha_2\tau})\cos(\omega_n\tau-\phi_n)d\tau-A_0\sum_{n=1}^{N_f}\int_0^{\infty}R_n(\mathrm{e}^{-\alpha_1\tau}-\mathrm{e}^{-\alpha_2\tau})\cos(\omega_n\tau-\phi_n)d\tau\right|\le M_2\\
&M_4(\omega)<\left|A_0\sum_{n=1}^{N_f}\int_0^{\infty}R_n(\mathrm{e}^{-\alpha_1\tau}-\mathrm{e}^{-\alpha_2\tau})\cos(\omega_n\tau-\phi_n)\,\mathrm{e}^{(-i\omega\tau)}\,d\tau\right|<M_3(\omega)
\end{aligned}\tag{3}$$

where $i=\sqrt{-1}$. It is clear that all constraints listed in Eq. (3) are nonlinear in nature. At first, a set of N_r earthquake records denoted by $\left\{\ddot{v}_{gi}(t)\right\}_{i=1}^{N_r}$ for the site under consideration are considered and then values of *E, PGA* and *PGV* are computed in each case. The largest of these values, across the ensemble of records, are taken to be the respective estimates for E, M_1 and M_2. In addition, the considered records are further normalized such that the Arias intensity of each record is set to unity ($\left[\int_0^{\infty}\ddot{v}_{gi}^2(t)\,\mathrm{d}t\right]^{\frac{1}{2}}=1$) and are denoted by $\left\{\ddot{\overline{v}}_{gi}(t)\right\}_{i=1}^{N_r}$. Therefore, the bounds $M_3(\omega)$ and $M_4(\omega)$ are obtained as (Moustafa 2011)

$$\begin{aligned}
M_3(\omega)&=E\max_{1\le i\le N_r}\left|\overline{v}_{gi}(\omega)\right|\\
M_4(\omega)&=E\min_{1\le i\le N_r}\left|\overline{v}_{gi}(\omega)\right|
\end{aligned}\tag{4}$$

Here $\left\{\overline{v}_{gi}(\omega)\right\}_{i=1}^{N_r}$ denotes the Fourier transform of $\left\{\ddot{\overline{v}}_{gi}(t)\right\}_{i=1}^{N_r}$. These procedures could be computed using the Fast Fourier Transform (FFT) as follows

$$\begin{aligned}
&\overline{v}_{gi}(\omega)=\int_0^{T^*}\ddot{v}_{gi}(t)e^{-i\omega t}dt=\int_0^{T^*}\ddot{v}_{gi}(t)\cos(\omega t)dt-i\int_0^{T^*}\ddot{v}_{gi}(t)\sin(\omega t)dt=A(\omega)-iB(\omega)\\
&\left|\overline{v}_{gi}(\omega)\right|=\sqrt{A^2(\omega)+B^2(\omega)}
\end{aligned}\tag{5}$$

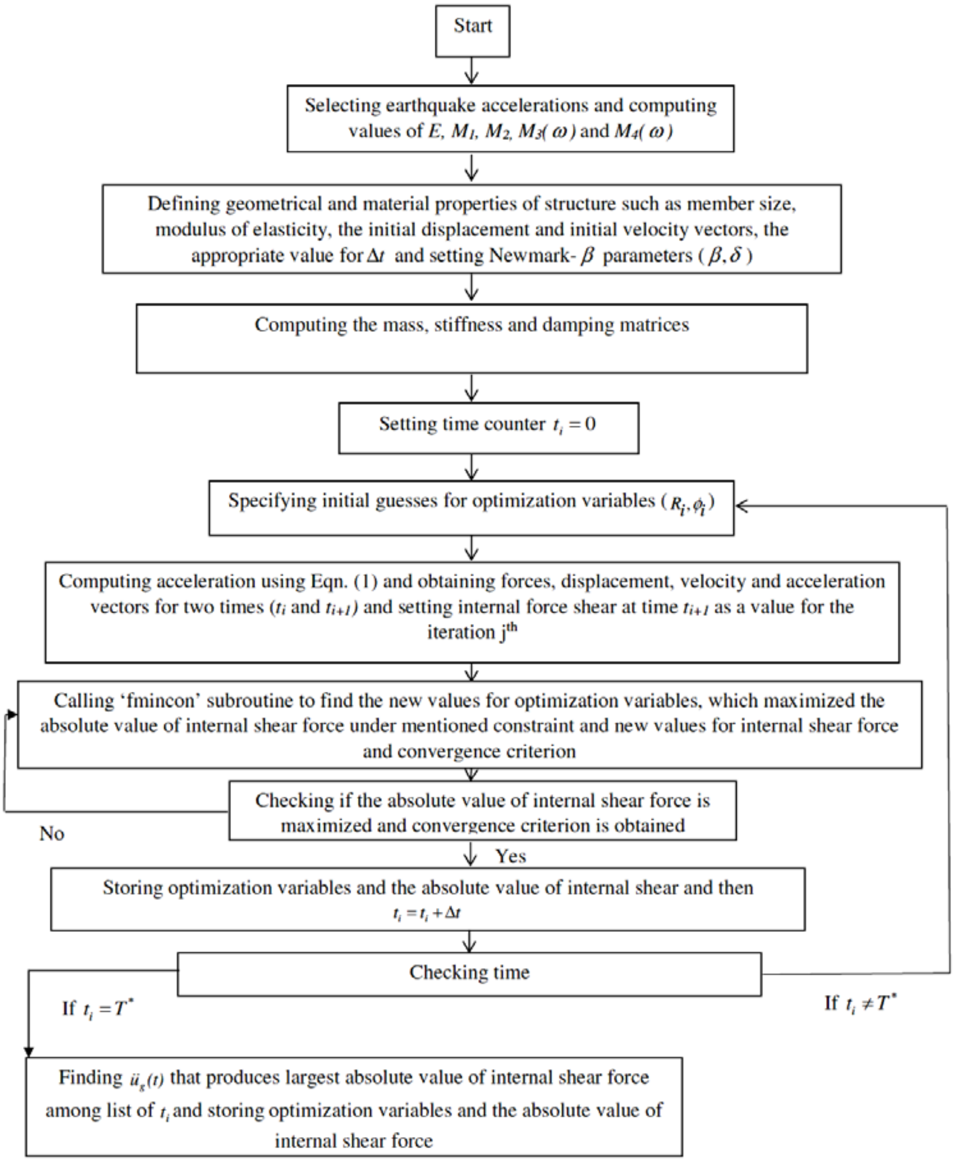

Fig. 1 Flowchart for deriving the maximum absolute value of internal shear force in design of important structures based on critical earthquake loads

The objective function maximizes the absolute value for internal shear force of the columns at the base of the structure. For purpose of demonstrating this procedure, a building strengthened by belt truss system is modeled as a two dimensional shear building subjected to lateral loading. Using time history analysis, critical excitation based on the constraints on ground motion at different times between (0-T^*) is computed so that the internal shear force is maximized. After performing the analysis, from the set of computed critical accelerations, one which produces the maximum internal shear force is selected. The solution to this nonlinear constrained optimization problem is tackled by using the sequential quadratic programming method (Arora 2012) and sequential quadratic optimization algorithm ‘fmincon’ of the Matlab optimization toolbox (Caleman *et al.* 1999). In the numerical calculations, alternative initial starting solutions, within the feasible region, were examined and were found to yield the same optimal solution. This was done for checking the local/global optimization (Takewaki *et al.* 2013). In this method, the following convergence criteria proposed by Moustafa (2011) were adopted

$$\left| f_j - f_{j-1} \right| \le \varepsilon_1; \qquad \left| y_{i,j} - y_{i,j-1} \right| \le \varepsilon_2 \tag{6}$$

Here f_j is the objective function at j^{th} iteration, $y_{i,j}$ is the i^{th} optimization variable at j^{th} iteration and $\varepsilon_1, \varepsilon_2$ are tolerance values to be specified. Absolute value of internal shear force is estimated using the Newmark β-method which is built as a subroutine inside the optimization program. Details of the procedure involved in computation of the critical earthquake are shown in Fig. 1.

It must be noted that the objective function can be defined as follows

$$f_j = -k_1 u_{1j} \tag{7}$$

where k_1 and u_{1j} are respectively the stiffness and displacement of the first storey at j^{th} iteration,. Eq. (7) shows that to maximize internal shear force at the base of the structure, it is necessary to find an acceleration which maximizes the relative displacement of the first storey.

3. Numerical example

A set of 14 earthquake ground motions is used to quantify the constraint bounds for $E, M_1, M_2, M_3(\omega)$ and $M_4(\omega)$ [Consortium of Organizations for Strong Motion Observation Systems COSMOS (2009)]. Table 1 provides information on these records. It should be emphasized that the selection of past records is primarily based on local soil conditions. Any new record that brings in changes to the value of constraints will automatically alter the critical response (Moustafa 2011). Differences in characteristics of recorded ground motions can lead to substantial differences in the structural response. According to Chandler’s 1991 classification, accelerograms are divided into three sets based on their (PGA/PGV) ratios. Records with PGA/PGV<0.8 g/(m/sec) are classified in low PGA/PGV range, whereas those with PGA/PGV >1.2 g/(m/sec) are classified as having high (PGA/PGV) ratios. Records with (PGA/PGV) between 0.8 and 1.2 g/(m/sec) are classified as the intermediate (PGA/PGV) range (Chandler *et al.* 1991).

In order, to provide a consistent approach, the classification noted above was used in this paper and three different (PGA/PGV) ratios from each category were incorporated.

The (PGA/PGV) ratios from 14 different earthquakes adopted in this paper are given in Table 1.The Fourier amplitude spectra for normalized acceleration (having unit Arias intensity) listed in Table 1, are computed and modified by SeismoSignal program. Based on these results, the upper and lower Fourier amplitude spectra is plotted in Fig. 2. In addition, four constraint scenarios that were considered in deriving the optimal earthquake inputs are listed in Table 2.

As an example, a twenty storey shear building (see Fig. 3) strengthened by a single belt truss system located in storey 18 is considered. A few studies exist which present optimum location of belt truss system under earthquake and wind loading to minimize the roof displacement (Raj Kiran

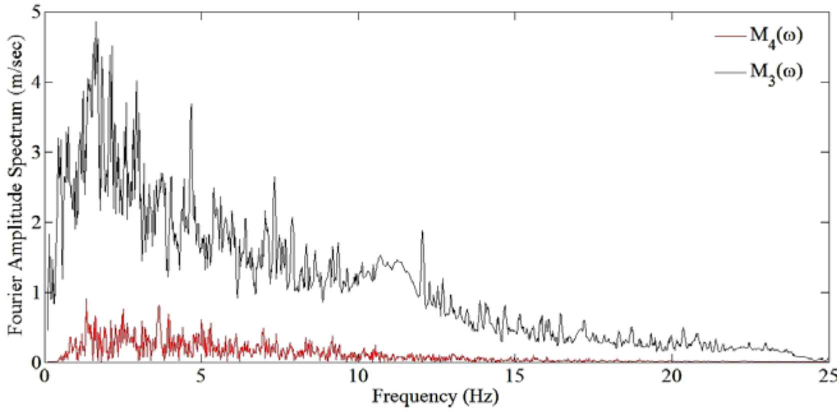

Fig. 2 Upper and lower bound of Fourier amplitude spectra for normalized acceleration

Nanduri *et al.* 2013, Herath *et al.* 2009). Also, there are a few literatures which present the optimum location of belt truss system subjected to static loading (Jahanshahi and Rahgozar 2013, Rahgozar and Sharifi 2009). In these mentioned papers, the optimum location of belt truss system for earthquake loading is variable depending on the stiffness of building and the earthquake loading between 0.5 to 1.0 times of building's height. In addition, in the mentioned literature, the optimum location of belt truss system subjected to static loading is variable between 0.4 to 0.7 times of building's height too. In this paper, the mentioned building is subjected to accelerations listed in Table 1 and the belt truss system is placed at each storey from bottom to the top storey. Then for each earthquake, the position of belt truss which minimizes the roof displacement is determined. For this purpose, the belt truss system is placed in a specific storey and the building is analyzed by time history analysis (Newmark-β method) subjected to the specific earthquake. From this analysis, the maximum roof displacement is determined. Then this process is repeated for other remained stories and finally amongst the maximum roof displacement, one of them which has the minimum roof displacement is selected as an optimum location for belt truss system. The optimum location of belt truss is between storey17 to storey 19 for nearly all listed earthquake in Table 1. For example, in Northridge earthquake, the optimum location of belt truss is storey 17 for S16W component and storey 19 for S74E component. This is valid for Mammoth Lakes earthquake too. Also, for strong ground motion listed in Table 1 such as Loma Prieta, Westmorland the storey 18 is the optimum location of belt truss system. Therefore, the storey 18 is selected as an optimum location for belt truss system to minimize the roof displacement.

Dimensions of exterior and interior columns of the building are shown in Fig. 3. All members of the belt truss system are the same and have cross sectional area of 0.0040 (m^2). Also, IPE 330 is used for all beam sections. Young's modulus and specific weight of the material are $19.906 \times 10^{10} (N / \mathrm{m}^2)$ and $76977.1\ (N / \mathrm{m}^3)$, respectively. The stiffness and mass matrices are formed and the damping matrix is computed such that the damping ratio for all modes would be 0.05. For this structure, the range of natural frequencies is from 2.12 to 138.16 (rad/sec). Fundamental natural period of the structure is 0.046 (sec) which renders the maximum Δt to be 0.0251 (sec) in order to ensure convergence and stability of the numerical time integration. In this example, the value of Δt is considered to be 0.005 (sec). In computation of the mass matrix, in addition to mass of the members, dead and live loads are considered to be 15444.45 (N/m) and

588.36 (N/m) respectively for all stories except for the roof. For roof, dead load is 12502.65 (N/m) and live load is 441.27 (N/m). The lumped mass, stiffness matrices and the force vector are presented in the appendix section.

Values of α_2 and α_1 are 0.50 and 0.13 respectively. This choice represents the earthquake duration (T^*) to be about 30 second. To select the number of frequency terms (N_f), a parametric study was carried out and $N_f = 90$ was found to be proper in order to obtain a better convergence for the critical acceleration and objective function (see Fig. 4).

Stiffness value of the belt truss system is computed as follows

$$k_{belt} = \sum_{n=1}^{N_b} \frac{AE}{L} \cos^2 \theta \tag{8}$$

where A, E, L, N_b and θ represent cross section, modulus of elasticity, length, number of members in the belt truss and angle of members for the belt truss as measured with respect to the horizontal line. It should be noted that only the stiffens of tensile members are computed. Also, since the belt truss system and storey are in parallel, stiffness of the belt truss is added to stiffness of the storey where belt truss is located at. For various types of belts used, the stiffness is taken from data given by Stafford Smith and Coull (1991).

Table 1 Information on past ground-motion records for firm soil site

Earthquake date	Magnitude	Epic.	Comp.	PGA	PGV	PGD	Energy*	PGA/PGV	Site
			Dist.×10^3 (m)	(m/s^2)	(m/s)	(m)	(m / s$^{1.5}$)	(g sec / m)	
Mammoth Lakes	6.2	1.5	90	4.02	0.22	0.05	3.73	1.86	Convict Greek
05.25.1980			180	3.92	0.23	0.05	4.02	1.74	
Loma Prieta	7.0	9.7	90	3.91	0.31	0.07	3.85	1.29	Capitola
10.18.1989			0	4.63	0.36	0.11	5.23	1.31	
San Fernando	6.6	27.6	N21E	3.09	0.17	0.04	2.08	1.85	Castaic Old Ridge
02.09.1971			N69W	2.65	0.28	0.10	2.48	0.96	
Parkfield	5.0	9.1	90	2.89	0.10	0.01	1.33	2.95	Parkfield fault
12.20.1994			360	3.80	0.09	0.007	1.74	4.3	
Northridge	6.7	5.9	S16W	3.81	0.60	0.12	4.19	0.65	Canoga Park
01.17.1994			S74E	3.43	0.34	0.09	3.52	1.03	
Westmorland	5.0	6.6	180	4.66	0.36	0.11	3.44	1.32	Westmorland fire
04.26.1981			90	3.77	0.44	0.13	3.30	0.87	
Imperial Valley	6.6	15.4	S45W	2.68	0.22	0.10	2.31	1.24	Calexico fire
10.15.1979			N45W	1.98	0.19	0.15	2.16	1.06	

$^{*}E=\left[\int_0^{\infty}\ddot{v}_g^2(t)\,\mathrm{d}t\right]^{\frac{1}{2}}$ (similar to Arias 1970)

Table 2 Nomenclature of constraint scenarios considered

Case	Constraint imposed
1	Energy and PGA
2	Energy, PGA and PGV
3	Energy, PGA and UBFAS
4	Energy, PGA, UBFAS and LBFAS

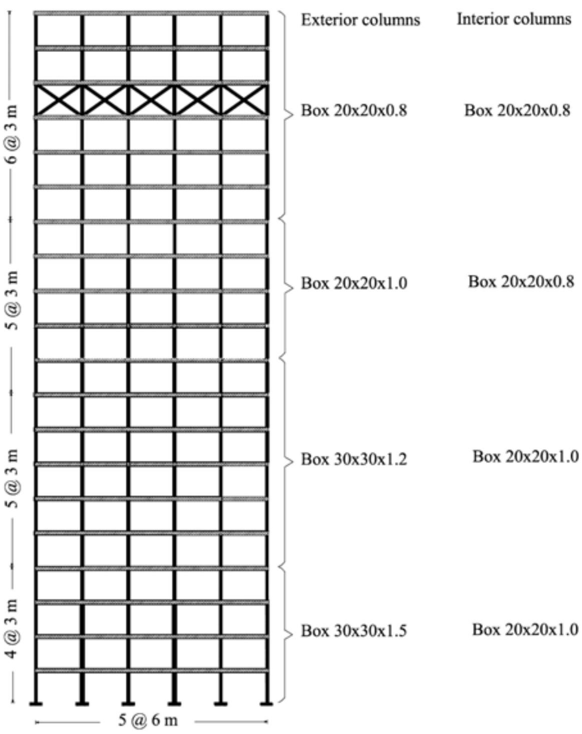

Fig. 3 The column sizes

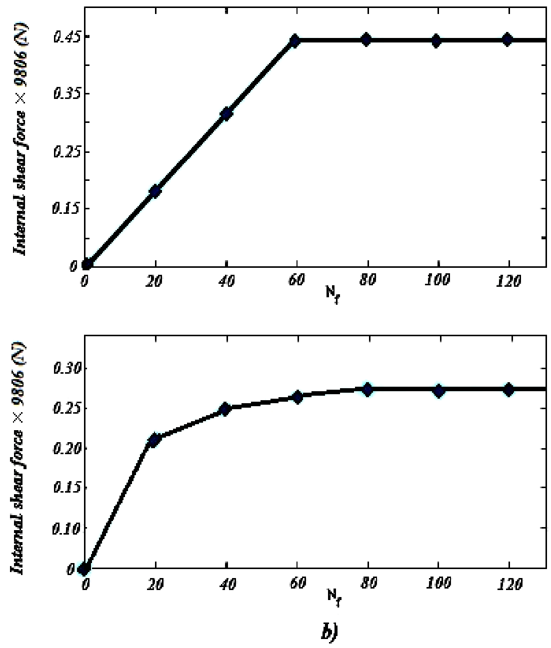

Fig. 4 Convergence of the objective function in terms of frequency terms N_f, (a) Case 1; (b) Case 4

The internal shear force is distributed between columns based on their stiffness. Therefore, for different cases, maximum absolute value of the internal shear force and maximum absolute value of the internal moment at their respective exterior column; along with the properties of computed critical excitation such as PGA, PGV, Arias intensity and PGA/PGV ratio are listed in Table 3. Furthermore, acceleration and velocity time histories as well as the Fourier spectra for various cases are shown in Fig. 5. Since, for cases one and two, there are no constraints on lower and upper bounds of the Fourier spectra, value of the Fourier spectra increases (see Fig. 5) till a frequency that coincides with natural elastic frequency of the structure is reached, thereby producing resonance.

Duration of critical accelerations for all cases based on Trifunac and Brady (1975) are shown in Fig. 5. From this figure, the duration for all cases is more than 12.86 (sec), (13.04, 13.38, 13.1 and 12.86 sec for all cases). Since the duration for strong ground motion, based on critical acceleration, are sufficiently large for all cases, these critical accelerations can be used for time history analysis of this structure based on UBC 97. It suggests that when appropriate recorded ground-motion time-history is not available, simulated ground-motion time-history can be used. In addition, if a group of critical excitations are computed for a specific structure, the computed accelerations can be used to obtain the response spectrum for the site at which the structure is located. Furthermore, this response spectrum can be used in design of that structure.

Table 3 Information on absolute value of internal shear force and absolute value of internal moment for one of the exterior columns under critical excitation for different cases

Case	Arias intensity	PGA	PGV	Shear force $\times 10^3$	Base moment $\times 10^3$	PGA/PGV
	($m/sec^{1.5}$)	(m/sec^2)	(m/sec)	(N)	(N. m)	(g sec/m)
1	5.23	4.1	3.4	433.52	233.09	0.123
2	4.57	3.94	0.60	338.21	181.80	0.670
3	3.66	3.98	0.38	227.11	122.08	1.068
4	3.31	3.63	0.40	202	108.55	0.9254

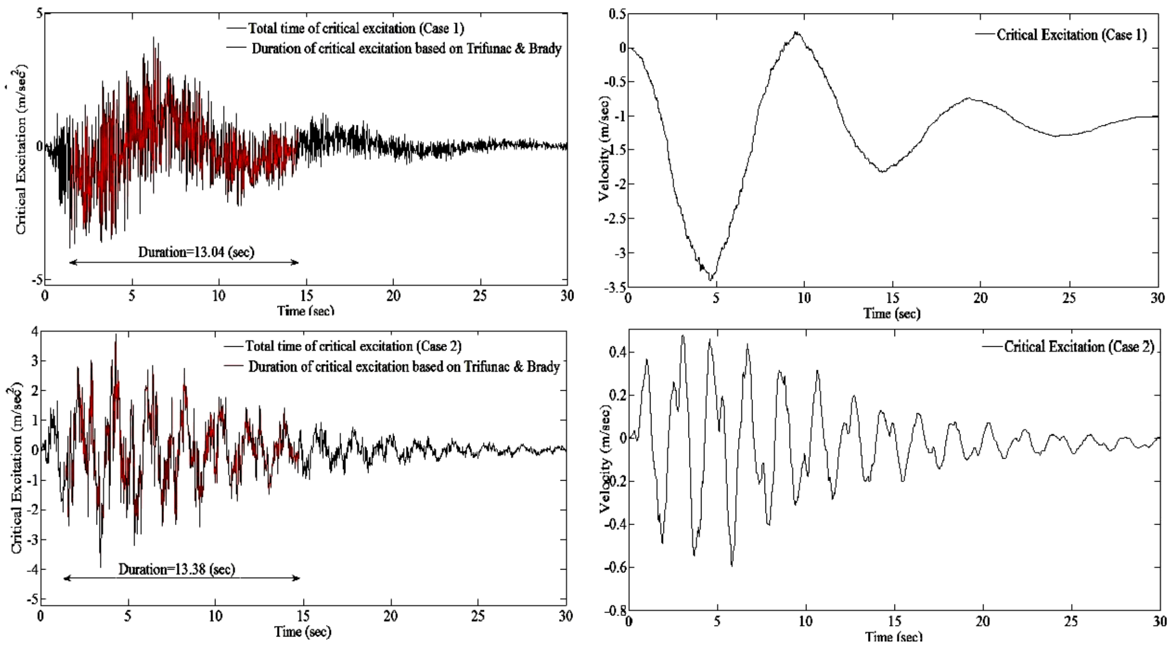

Fig. 5 Acceleration and velocity time histories, and Fourier spectra of critical excitation for different cases

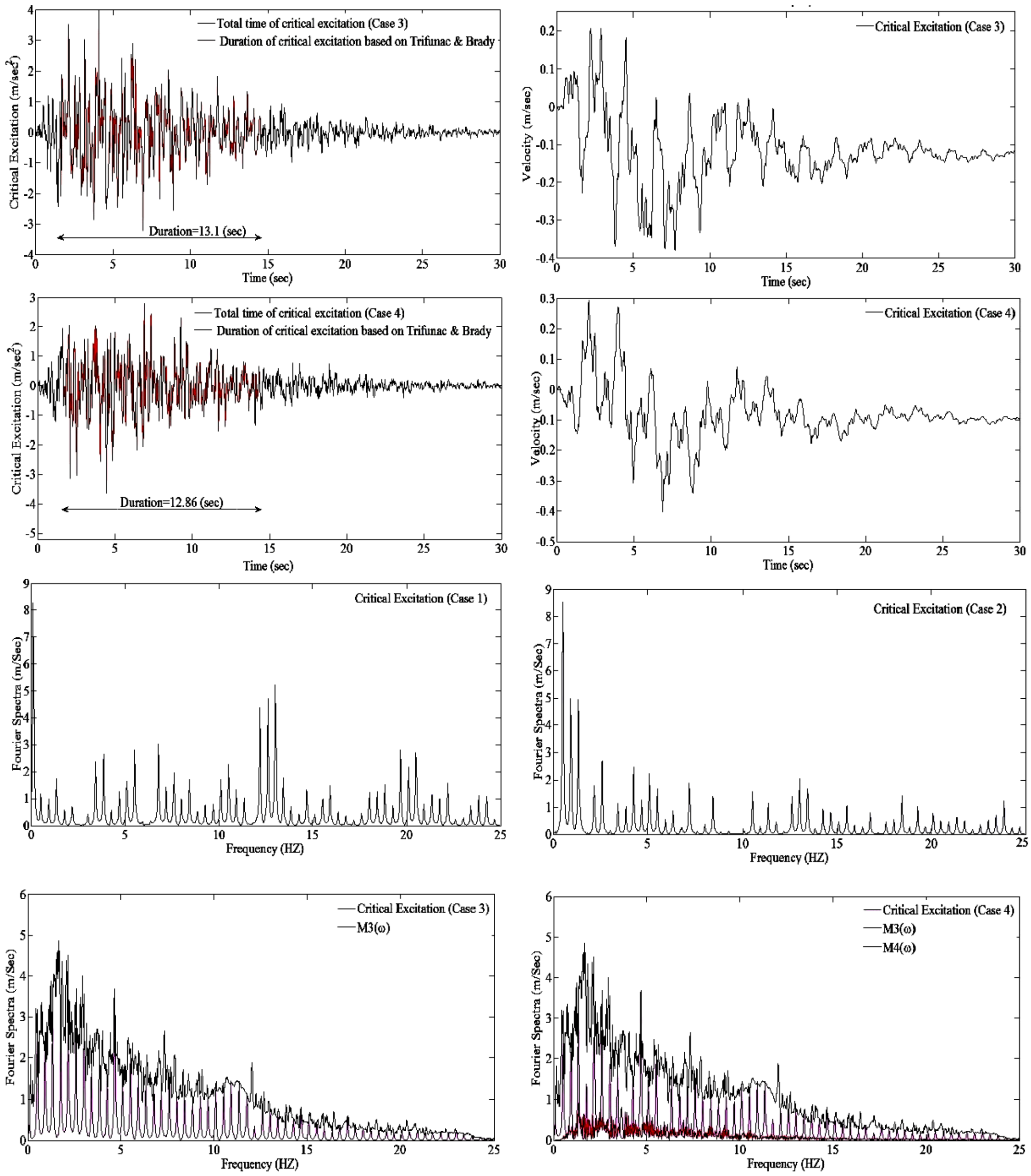

Fig. 5 Continued

4. Discussion

Based on numerical results, the following conclusions are reached:

1- The frequency content and Fourier amplitude of the critical acceleration are strongly dependent on the constraints imposed. If available information on earthquake data is limited to the total energy and PGA, the output is narrow band (highly resonant) and the internal shear force is conservative (see Fig. 5 and Table 3). Furthermore, for cases 1 and 2, as shown in Fig. 5, largest Fourier amplitude is at a frequency close to natural frequency of the elastic structure when the belt truss system is located at storey 18 ($f = 0.337(Hz)$) while the Fourier amplitudes at other frequencies are low. In addition, by applying additional constraints on the Fourier amplitude spectra in cases 3 and 4, the Fourier amplitude of the critical acceleration will be distributed across other frequencies. The critical acceleration possesses a dominant frequency that is close to the average dominant frequency observed in past records (see Fig. 5). This result matches well with earlier work reported by Moustafa (2011).

2- The absolute value of internal shear force for case 4 is 202×10^3 (N) which is substantially smaller than 433.52×10^3 (N) for case 1 (Table 3). The constraints on UBFAS and LBFAS were found to be significant in producing realistic critical inputs. Also, validity of the desired acceleration for case 4 can be examined by comparing the Fourier amplitude spectra and frequency content of the design acceleration (Fig. 5) with the Fourier amplitude spectra of recorded earthquakes.

3- Constraint scenarios 1 and 2 lead to pulse like ground motion which has been observed during some recent earthquakes (e.g., 1971 San Fernando and 1985 Mexico). These earthquakes are observable in near-field ground motion with directivity focusing (forward- and backward directivity) which have fault-parallel and fault-normal components (Kalkan and Kunnath 2006, He and Agrawal 2008, Moustafa 2011). Realism of optimal earthquake loads and hence the optimum internal shear force can also be examined by comparing maximum response from optimal accelerations with those from past recorded ground motions (see Table 3). Thus, maximum internal shear force of the structure based on design earthquake is about 2.78 (case 1) and 1.29 (case 4) times the San Fernando earthquake.

4- As shown in Table 3, the PGA/PGV ratio of the critical earthquake in cases 1-4 are 0.123, 0.670, 1.068 and 0.9254. These values place critical accelerations at low Chandler’s classification, low Chandler’s classification, intermediate Chandler’s classification and intermediate Chandler’s classification, respectively. As shown in this table, for case 1 that produces the maximum internal shear force and a pulse like ground motion, the PGA/PGV ratio is very low and places in low Chandler’s classification. Nevertheless, for cases 3 and 4 with the highest PGA/PGV ratio, the minimum internal shear force is produced. Since the highest value of PGV from past ground motion is selected as the constraint value, the denominator of PGA/PGV is increased leading to decrease in value of PGA/PGV. This result is also valid for internal moments.

5- As shown in Table 3 and Fig. 5, frequency content and Fourier amplitude of the design earthquake are more important factors than PGA and PGV. In cases (1) and (2), Fourier amplitude of the critical earthquake is concentrated at a frequency close to natural frequency of the elastic structure and leads to pulse like ground motion.

6- As mentioned earlier, the duration of computed critical excitation is large enough, hence, a group of critical excitations can be used to build the response spectrum in design of special structures.

In fact, the critical excitation method is a robustness tool that can be used to produce the resonant or critical acceleration in designing important structures. If there is no recorded acceleration for a given site, this method can be used to construct a group of acceleration in designing of important building which are going to be design in this region. In addition, the critical excitation method produces the critical excitation that can only be used for the structures that has been used in the formulation and accelerations have produced for it based on the properties such as mass, damping and stiffness matrices. These accelerations can be utilized approximately for a similar building with analogous first natural frequency with the analyzed building by critical excitation method. As a disadvantage of this method, the critical excitation method is time consuming and it is better to be used for important structures with high safety conditions under severe earthquake.

5. Conclusions

In this paper, critical excitation method was used to find maximum absolute value of internal shear force and moment, required in design of important structures which must remain without damage or with a little damage after a severe earthquake. Critical acceleration is estimated on the basis of available information using inverse dynamic analysis and nonlinear optimization methods. To demonstrate the process, a building which was strengthened by a system of belt truss was considered and modeled as a two dimensional shear building. The belt truss system is placed at 18th storey and using time history analysis, the critical excitation based on the constraints on ground motion at different times between (0-T^*) is computed so that the internal shear force is maximized. From the set of computed critical accelerations, one of them which produces the maximum internal shear force is selected. It is found that if available information is limited to the energy and PGA (case 1) or energy, PGA and PGV (case 2), the resulting earthquake is highly resonant and produces conservative internal shear force. Since in cases (3) and (4), the amplitude Fourier spectra is constrained, the resulting earthquakes have low value for internal shear force. These two scenarios (cases 3 and 4) can be used for less important structures or for regions that the resonant earthquake cannot occur. The proposed method is simple and efficient in determining the maximum internal shear force for design of important structures. In addition, since these types of acceleration have important effect on important structures, one can use a group of them to build a response spectrum to be used for design of important buildings. The numerical example shows the efficiency of the proposed method.

References

Abbas, A.M. (2006), "Critical seismic load inputs for simple inelastic structures", *J. Sound. Vib.*, **296**, 949-67.

Abbas, A.M. and Manohar, C.S. (2002), "Critical spatially-varying earthquake load models for extended structures", *J. Struct. Eng*., ASCE, **29**(1), 39-52.

Anderson, J.C. and Bertero, V.V. (1987), "Uncertainties in establishing design earthquakes", *J. Struct. Eng*., ASCE, **113**(8), 1709-1724.

Arias, A. (1970), A measure of earthquake intensity: seismic design for nuclear power plants, MIT Press, Cambridge, MA.

Arora, J.S. (2012), *Introduction to Optimum Design*, Elsevier, Academic Press, USA.

Caleman, T., Branch, M.A. and Grace, A. (1999), *Optimization Toolbox for the Use with Matlab: User's Guide*, The Math Works Inc., USA.

Chandler, A.M., Pappin, J.W. and Coburn, A.W. (1991), "Vulnerability and seismic risk assessment of buildings following the 1989 Newcastle, *Australia earthquake*", *Bull. NZ. Soc. Earthq. Eng*., **24**(2), 116-138.

COSMOS (2009) Consortium organizations for strong-motion observation systems. http://www.strongmotioncenter.org/vdc/scripts/default.plx

Drenick, R.F. (1970), “Model-free design of aseismic structures”, *J. Eng. Mech*., ASCE, **96**(4), 483-493.

Drenick, R.F. (1977), On a class of non-robust problems in stochastic dynamics, Stochastic Problems in Dynamics, Ed., B.L. Clarkson, Pitman, London.

Fujita, K. Kasagi, M. Lang, Z.Q. Penfei, G. and Takewaki, I., (2014), “Optimal Placement and design of nonlinear dampers for building structures in the frequency domain”, *Earthq. Struct*., **7**(6), 1025-1044.

He, W.L. and Agrawal, A.K. (2008), “Analytical model of ground motion pulses for the design and assessment of seismic protective systems”, *J. Struct. Eng*., ASCE, **134**(7), 1177-1188.

Heidari, A., Rahgozar, R. and Kamgar, R. (2014), “Free vibration analysis of tall building with geometrical discontinuities”, *Acia. J. Civil. Eng.*, **15**(1), 107-122.

Herath, N., Haritos, N., Ngo, T. and Mendis, P. (2009), “Behavior of outrigger beams in high-rise buildings under earthquake loads, *Aust. Earthq. Eng. Soc.*, Australia.

Jahanshahi, M.R., Rahgozar, R. and Malekinejad, M. (2012), “A simple approach to static analysis of tall buildings with a combined tube-in-tube and outrigger-belt truss system subjected to lateral loading”, *Int. J. Eng. Trans. A: Basic.*, **25**(3), 289-299.

Jahanshahi, M.R. and Rahgozar, R. (2013), “Optimum location of outrigger-belt truss in tall buildings based on maximization of the belt truss strain energy”, *Int. J. Eng. Trans. A: Basics.*, **26**(7), 693-700.

Kalkan, E. and Kunnath, S.K. (2006), “Effects of fling step and forward directivity on seismic response of buildings”, *J. Earthq. Spectra*., **22**(2), 367-390.

Kamgar, R. and Rahgozar, R. (2013), “A simple approximate method for free vibration analysis of framed tube structures”, *Struct. Des. Tall. Spec*., **22**(2), 217-234.

Kamgar, R. and Saadatpour, M.M. (2012), “A simple mathematical model for free vibration analysis of combined system consisting of framed tube, shear core, belt truss and outrigger system with geometrical discontinuities”, *Appl. Math. Model*., **36**(10), 4918-4930.

Kuang, J.S. and Ng, S.C. (2004), “Coupled vibration of tall buildings structures”, *Struct. Des. Tall. Spec*., **13**(4), 291-303.

Malekinejad, M. and Rahgozar, R. (2014), “An analytical model for dynamic response analysis of tubular tall buildings”, *Struct. Des. Tall. Spec*., **23**(1), 67-80.

Moustafa, A. (2009), “Critical earthquake load inputs for multi-degree-of-freedom inelastic structures”, *J. Sound. Vib.*, **325**(3), 532-544

Moustafa, A. (2011), “Damage-based design earthquake loads for single-degree-of-freedom inelastic structures”, *J. Struct. Eng*., ASCE., **137**(3), 456-467.

Moustafa, A. (2012), *Earthquake-Resistant Structures: Design, Assessment and Rehabilitation*, InTech, Croatia, Italy.

Rahgozar, R. and Sharifi, Y. (2009), “An approximate analysis of combined system of framed tube, shear core and belt truss in high-rise buildings”, *J. Struct. Des. Tall. Spec*., **18**(6), 607-624.

Rahgozar, R., Mahmoudzadeh, Z., Malekinejad, M. and Rahgozar, P. (2014), “Dynamic analysis of combined system of framed tube and shear walls by Galerkin method using B-spline functions”, *J. Struct. Des. Tall. Spec*., doi: 10.1002/tal.1201.

Raj Kiran Nanduri, P.M.B., Suresh, B. and Ihtesham Hussain, M.D. (2013), “Optimum position of outrigger system for high-rise reinforced concrete buildings under wind and earthquake loadings”, *Am. J. Eng. Res*., **2**(8), 76-89.

SeismoSignal 5.1.0 2013, Seismosoft Ltd., Pavia, Italy.

Shinozuka, M. (1970), “Maximum structural response to seismic excitations”, *J. Eng. Mech*., ASCE, **96**(5), 729-738.

Shinozuka, M. and Sato, Y. (1967), “Simulation of nonstationary random process”, *J. Eng. Mech*., ASCE, **93**(1), 11-40.

Singh, J.P. (1984), “Characteristics of near-field ground motion and their importance in building design, ATC-10-1 Critical aspects of earthquake ground motion and building damage potential”, *ATC*, 23-42.

Stafford Smith, B. and Coull, A. (1991), *Tall Building Structures: Analysis and Design*, John Willey, New York, USA.

Stein, R.S. (2003), “Earthquake conversations”, *Sci. Am*., **288**(1), 72-79.

Swaddiwudhipong, S., Soelarno Sidji, S. and Lee, S.L. (2002), "The effects of axial deformation and axial force on vibration characteristics of tall buildings", *J. Struct. Des. Tall. Spec*., **11**(5), 309-328.
Takewaki, I. (2001a), "A new method for non-stationary random critical excitation", *Earthq. Eng. Struct. Dyn*., **30**(4), 519-535.
Takewaki, I. (2001b), "Nonstationary random critical excitation for acceleration response", *J. Eng. Mech*., ASCE, **127**(6), 544-556.
Takewaki, I. (2002), "Seismic critical excitation method for robust design: A review", *J. Struct. Eng*., ASCE, **128**(5), 665-672.
Takewaki, I., (2005), "Bound of earthquake input energy to soil-structure interaction systems", *Soil. Dyn. Earthq. Eng.*, **25**(7-10), 741-752.
Takewaki, I. (2013), *Critical Excitation Methods in Earthquake Engineering*, Elsevier, Netherlands.
Takewaki, I., Moustafa, A. and Fujita, K. (2013), *Improving the Earthquake Resilience of Buildings, the Worst Case Approach*, Springer, London.
Takewaki, I. (2013), "Toward greater building earthquake resilience using concept of critical excitation: A review", *J. Sustain. City. Soc*., **9**, 39-53.
Taranath, B.S. (2012), *Structural Analysis and Design of Tall Buildings: Steel and Composite Construction*, Taylor & Francis, CRC Press, New York, USA.
Trifunac, M.D. and Brady, A.G. (1975), "A study on the duration of strong earthquake ground motion", *Bull. Seismol. Soc. Am.*, **65**(3), 581-626.
Uniform Building Code (1997), *International Conference of Building Officials*, Whittier, California, USA.
Westermo, B.D. (1985), "The critical excitation and response of simple dynamic systems", *J. Sound Vib*., **100**(2), 233-242.
Wu, J.R. and Li, Q.S. (2003), "Structural performance of multi-outrigger braced tall buildings", *J. Struct. Des. Tall. Spec*., **12**(2), 155-176.

CC

Appendix: Mass, stiffness matrices and the force vector

The lumped mass, stiffness matrices and the force vector for mentioned building in the numerical example are as follows:

a) Lumped mass matrix:

$[M]=[M]_{20\times 20}$
$M_{i,j}=0$ If $i\neq j$
$M_{1,1}=M_{2,2}=M_{3,3}=5.1992 * 10^4$ ($N\ sec^2/m$); $M_{4,4}=5.1914 * 10^4$ ($N\ sec^2/m$)
$M_{5,5}=M_{6,6}=M_{7,7}=M_{8,8}=5.1837 * 10^4$ ($N\ sec^2/m$); $M_{9,9}=5.1691 * 10^4$ ($N\ sec^2/m$)
$M_{10,10}=5.1480 * 10^4$ ($N\ sec^2/m$);
$M_{11,11}=M_{12,12}=M_{13,13}=5.1412 * 10^4$ ($N\ sec^2/m$);
$M_{14,14}=5.1378 * 10^4$ ($N\ sec^2/m$);
$M_{15,15}=M_{16,16}=M_{17,17}=M_{19,19}=5.1343 * 10^4$ ($N\ sec^2/m$);
$M_{18,18}=5.3426 * 10^4$ ($N\ sec^2/m$); $M_{20,20}=4.1459 * 10^4$($N\ sec^2/m$)

b) Stiffness matrix:

$[K]=[K]_{20\times 20}$
$K_{i,j}=K_{i,j}$
$K_{1,1}=K_{2,2}=K_{3,3}=1.1460 * 10^8$ (N/m);
$K_{4,4}=1.074 * 10^8$ (N/m); $K_{5,5}=K_{6,6}=K_{7,7}=K_{8,8}=1.002 * 10^8$ (N/m);
$K_{9,9}=0.7444 * 10^8$ (N/m); $K_{10,10}=0.4584 * 10^8$ (N/m);
$K11,11=K_{12,12}=K_{13,13}=0.4299 * 10^8$ (N/m);
$K_{14,14}=0.4157 * 10^8$ (N/m);
$K_{15,15}=K_{16,16}=K_{19,19}=0.4015 *10^8$ (N/m);
$K_{17,17}=K_{18,18}=5.0958 * 10^8$ (N/m);
$K_{20,20}=0.2007 * 10^8$ (N/m);
$K_{1,2}=K_{2,3}=K_{3,4}=-0.5730 * 10^8$ (N/m);
$K_{4,5}=K_{5,6}=K_{6,7}=K_{7,8}=K_{8,9}=-0.501 * 10^8$ (N/m);
$K_{9,10}=-0.2434 * 10^8$ (N/m);
$K_{10,11}=K_{11,12}=K_{12,13}=K_{13,14}=-0.2150 * 10^8$ (N/m);
$K_{14,15}=K_{15,16}=K_{16,17}=K_{18,19}=K_{19,20}=-0.2007 * 10^8$ (N/m);
$K_{17,18}=-4.8950 * 10^8$ (N/m);
$K_{1,3}=K_{1,4}=\ldots=K_{1,20}=0$ (N/m); $K_{2,4}=K_{2,5}=K_{2,20}=0$ (N/m);
$K_{3,5}=K_{3,6}=\ldots=K_{3,20}=0$ (N/m); $K_{4,6}=K_{4,7}=\ldots=K_{4,20}=0$ (N/m);
$K_{5,7}=K_{5,8}=\ldots=K_{5,20}=0$ (N/m); $K_{6,8}=K_{6,9}=\ldots=K_{6,20}=0$ (N/m);
$K_{7,9}=K_{7,10}=\ldots=K_{7,20}=0$ (N/m); $K_{8,10}=K_{8,11}=\ldots=K_{8,20}=0$ (N/m);
$K_{9,11}=K_{9,12}=\ldots=K_{9,20}=0$ (N/m); $K_{10,12}=K_{10,13}=\ldots=K_{10,20}=0$ (N/m);
$K_{11,13}=K_{11,14}=\ldots=K_{11,20}=0$ (N/m); $K_{12,14}=K_{12,15}=\ldots=K_{12,20}=0$ (N/m);
$K_{13,15}=K_{13,16}=\ldots=K_{13,20}=0$ (N/m); $K_{14,16}=K_{14,17}=\ldots=K_{14,20}=0$ (N/m);
$K_{15,17}=K_{15,18}=\ldots=K_{15,20}=0$ (N/m); $K_{16,18}=K_{16,19}=\ldots=K_{16,20}=0$ (N/m);
$K_{17,19}=K_{17,20}=0$ (N/m); $K_{18,20}=0$ (N/m)

c) Force vector:

The equation of motion for structure subjected to critical excitation is

$$\left[M\right]\left\{\ddot{x}\right\}+\left[C\right]\left\{\dot{x}\right\}+\left[K\right]\left\{x\right\}=-\left[M\right]\left\{1\right\}\ddot{u}_g(t) \tag{A-1}$$

where $\left[M\right]$, $\left[C\right]$ and $\left[K\right]$ are the mass, damping and stiffness matrices, respectively; $\left\{\ddot{x}\right\}$, $\left\{\dot{x}\right\}$ and $\left\{x\right\}$ are the acceleration, velocity and displacement vectors of the structure respectively and $\left\{1\right\}$ is a vector with each element equal to unity. $\ddot{u}_g(t)$ shows the ground acceleration that is defined in Eq. (1). Therefore in Eq. (A-1), $-\left[M\right]\left\{1\right\}\ddot{u}_g(t)$ represents the force vector that applied to the structure in time *t*.